JOURNAL OF CATALYSIS 60, 41–56 (1979)

Platinum-Catalyzed Gasification of Graphite by Hydrogen[1]

D. R. OLANDER AND M. BALOOCH

Materials and Molecular Research Division of the Lawrence Berkeley and the Department of Nuclear Engineering, University of California, Berkeley, California 94720

Received January 25, 1979; revised March 26, 1979

The production of methane by reaction of molecular hydrogen with partially platinum-covered graphite was studied by the modulated molecular beam method. Although molecular hydrogen does not react with pure graphite at temperatures <800 K, deposition of the equivalent of several monolayers of platinum on the surface results in significant gasification rates. The platinum deposits as islands several monolayers thick separated by uncovered graphite. The reaction appears to occur by dissociative adsorption of H_2 on the platinum zones followed by spill-over of H atoms to the graphite zones where methane production takes place. A detailed mechanism based on this model was applied to the molecular beam data and permitted determination of the sticking coefficient and recombination rate constant of hydrogen on the platinum zones, and the reaction rate constants and surface diffusion coefficient of hydrogen on the exposed graphite surface.

I. INTRODUCTION

Molecular hydrogen reacts very slowly with pyrolytic graphite. In the previous molecular beam study of this system (*1*), no reaction could be detected with H_2 as the reactant gas. However, when the hydrogen was thermally dissociated prior to striking the graphite surface, substantial reaction occurred. The difference in graphite reactivity between the molecular and atomic forms of hydrogen is due to the very low dissociative sticking probability of H_2 on graphite. Atomic hydrogen, on the other hand, exhibits a sticking probability of 0.006 on the basal plane of pyrolytic graphite and 0.02 on the prism plane (*1*). At low temperatures, methane is the sole of the C/H product reaction. The yield of CH_4 decreases rapidly with temperature above about 700 K because surface recombination of adsorbed H atoms to form H_2 becomes significant. In addition to these two surface chemical processes, the C/H reaction was found to be strongly influenced by solution and diffusion of hydrogen atoms in the bulk of the solid.

The present investigation was designed to determine if instead of thermally dissociating the H_2 gas, a metal deposit on the surface could serve as a source of H atoms for gasification of the graphite. Platinum was used because of its demonstrated ability to chemisorb hydrogen with a high sticking probability (*2–5*) and because of its technological significance as a catalyst for many chemical reactions.

II. EXPERIMENTAL

The same type of pyrolytic graphite specimens were used for the C/Pt/H_2

[1] This work was supported by the Division of Basic Energy Sciences of the Department of Energy under contract No. W-7405-Eng-48.

0021-9517/79/130041-16$02.00/0

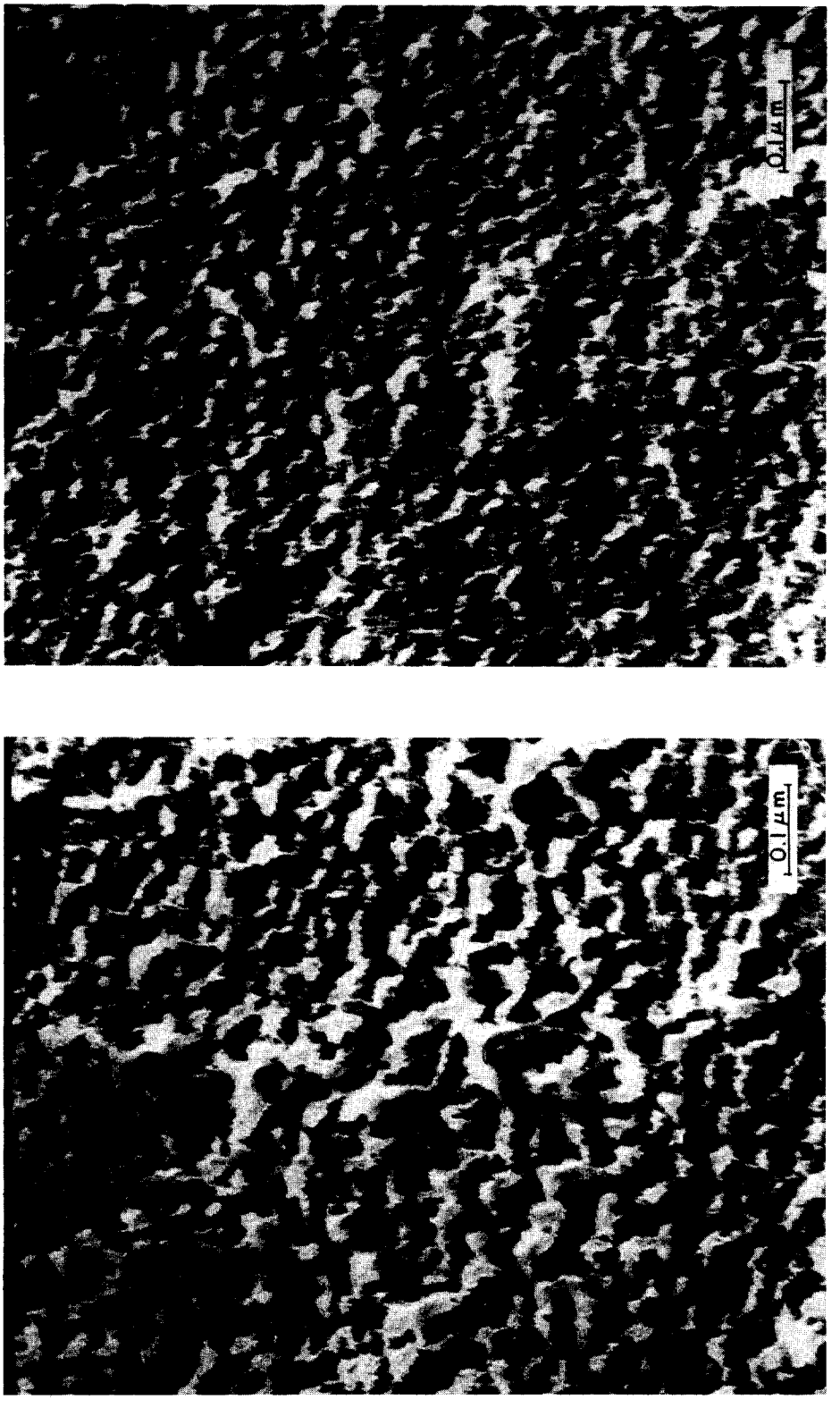

FIG. 1. Replica electron micrographs of polished graphite surfaces after coating with four equivalent monolayers of platinum.

study as was employed in the previous C/H study (*1*). The Union Carbide Co. supplied the graphite as wafers (15 mm in diameter and 3 mm thick) which had been annealed at 3000°C for several hours. The faces of one wafer consisted of basal planes and, in the other specimen, the faces were prism planes. The samples were >99.5% of theoretical density and contained <1 ppm of metallic impurities as determined by neutron activation analysis. Metal was deposited on the graphite surface held in vacuum at 400°C by vaporization from a heated platinum filament. The rate of impingement of platinum atoms on the graphite surface was determined from the filament temperature by means of the Hertz–Langmuir equation. The evaporation time was varied to produce platinum coverages ranging from one to five monolayers (if the deposits were uniform). Replica electron micrographs of graphite surfaces coated with four equivalent monolayers of platinum are shown in Fig. 1. Instead of uniform layer formation, islands of the metal (the black areas in Fig. 1) formed on the graphite (white zones). On the prism plane specimen shown in Fig. 1, the platinum deposit occupied about one-half of the total surface area, which means that the average thickness of the discrete platinum zones was ~eight monolayers. The metal aggregated in the form of strips averaging about 200 Å wide. The platinum evaporated onto the basal plane surfaces produced larger coverages for the same exposure to Pt vapor. At a coverage of four effective monolayers, platinum covers about two-thirds of the surface, leaving graphite strips ~100 Å wide. Prior to conducting the reaction study on these surfaces, an attempt was made to remove carbon from the platinum deposits by exposing the specimens to 6×10^{-5} Torr of oxygen at 850°C for 0.5 hr.

The deposition process and the reaction study were conducted in the molecular beam apparatus shown in Fig. 2. A molecular beam of hydrogen is generated by effusion from a room-temperature source tube containing a 1-mm orifice at one end. The flux from this hole is mechanically modulated by a rotating slotted disk, the frequency of modulation being measured by a light-photodiode arrangement which is triggered by the rotating blades of the chopper. The chopped flow of low-density gas is formed into a beam by collimating with a 1-mm-diameter orifice separating the source chamber from the target chamber. This beam impinges on the target at an angle of 45°. Scattered (and desorbed) H_2 and the methane reaction product are detected in direct flight from the target by the quadrupole mass spectrometer located in the detector chamber of Fig. 2, which communicates with the source chamber via a 2-mm-diameter orifice. The modulated product and reactant signals are processed by lock-in amplification to yield the apparent reaction probability (the ratio of the amplitudes of the product and reactant signals, corrected for ionization efficiencies of the mass spectrometer) and the phase lag, which is the difference between the product and the reactant phase angles. These two quantities were measured as functions of target temperature T, modulation frequency ω, and incident beam intensity I_0 (the amplitude of the square-chopped beam). The experimental program consisted of choosing reference conditions (denoted by asterisks):

$$\omega^* = 54 \text{ Hz}$$

$$I_0^* = 3 \times 10^{17} \text{ molecules/cm}^2\text{-sec}$$

$$T^* = 683 \text{ K}$$

and changing one variable at a time. The three sets of experiments in this program were:

frequency scan: $1 < (\omega/\omega^*) < 16$ at I_0^* and T^*

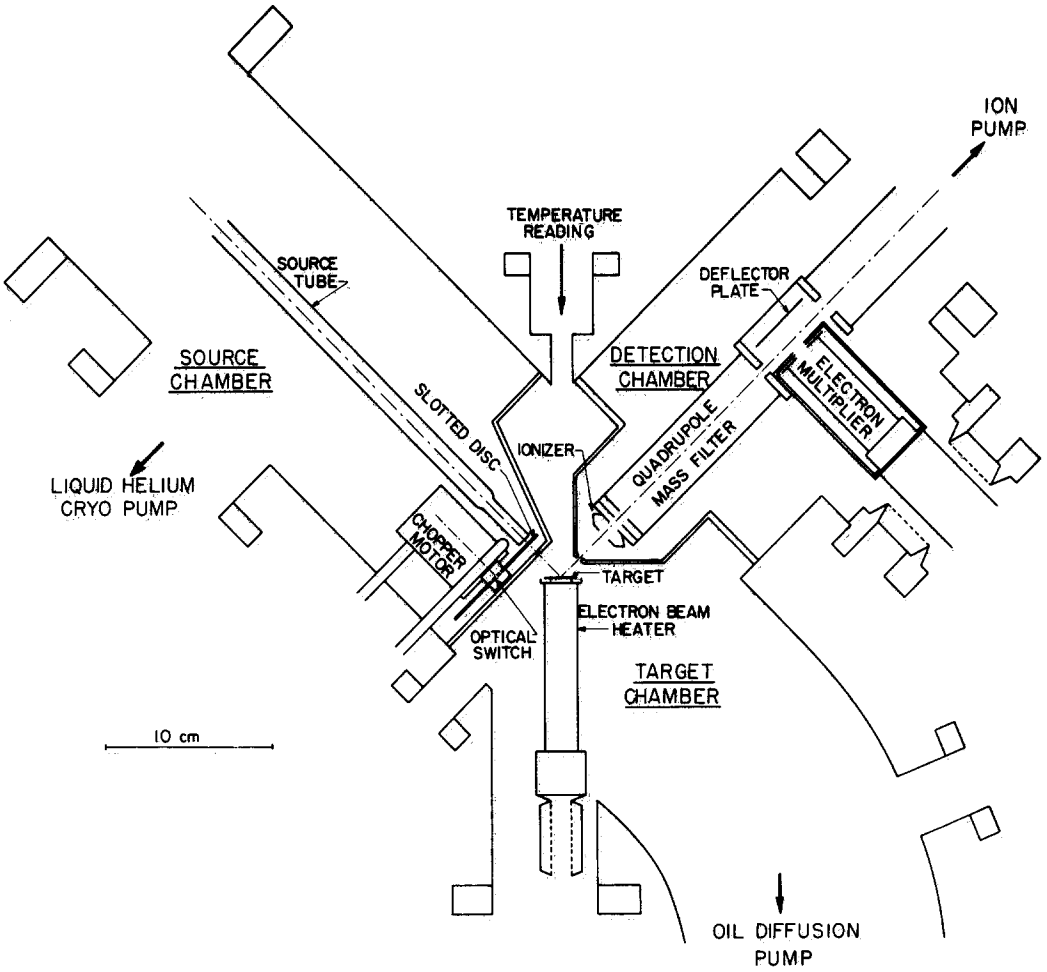

FIG. 2. Schematic of the molecular beam apparatus.

beam intensity variation: $0.1 < (I_0/I_0^*) < 2$ at ω^* and T^*

temperature variation: 530 K $< T <$ 840 K at ω^* and I_0^*

In addition, the following measurements were made under the reference conditions:

(i) effect of amount of platinum deposited (one to five equivalent monolayers),

(ii) effect of poisoning. The reaction probability was followed for several hours until it began to decrease. The platinum surface was then reactivated by a brief oxygen treatment.

The above experiments were conducted on both the basal and prism orientations of the graphite samples.

III. RESULTS

Figure 3 shows the apparent reaction probability as a function of platinum coverage at reference reaction conditions. Without platinum on the surface, no reaction is detectable. Reactivity increases as more platinum is deposited and passes through a maximum at a coverage of four equivalent monolayers. The maximum reaction probability observed is 10^{-4}, which is a factor of 50 smaller than the largest reaction probability measured in the C/H investigation (*1*). In the platinum-cata-

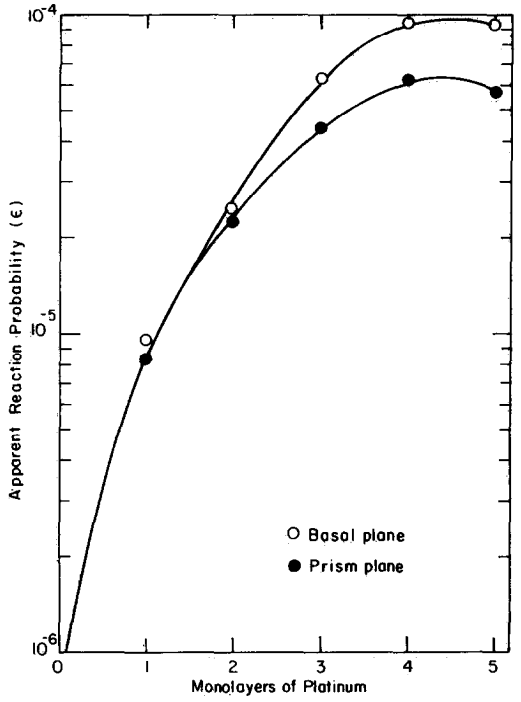

FIG. 3. Effect of platinum coverage on the reaction probability for reference reaction conditions.

lyzed system, the basal plane is more reactive than the prism surface, which is the opposite of the order found in graphite gasification by atomic hydrogen, oxygen, and water vapor.

Qualitatively, the explanation of the behavior shown in Fig. 3 is straightforward. At low platinum coverages, reaction efficiency is limited by the quantity of metal needed to dissociate inpinging H_2 molecules and thereby supply the H atoms to the graphite for gasification. At high coverages, such a large fraction of the available surface is covered with metal that the remaining graphite cannot produce sufficient methane for a high reaction probability even though hydrogen is readily available from the platinum zones. Obviously, at very large platinum coverage, the reaction probability must be zero because no graphite is exposed to the beam. The optimum under our reaction conditions is four equivalent monolayers, which corresponds to surfaces containing 50 and 33% exposed graphite for the prism and basal planes, respectively (see Fig. 1).

Figure 4 shows that the platinum deposits lose their catalytic activity after 10 to 100 min of reaction. The surfaces with the highest platinum coverages keep their reactivity the longest. This observation suggests that the poisoning process involves diffusion of carbonaceous species from the graphite surface on top of the

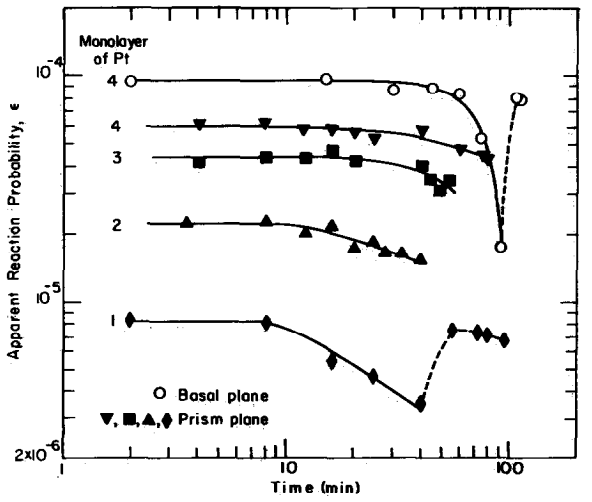

FIG. 4. Degradation of reactivity with time under reference reaction conditions. The dashed portions of the upper and lower curves represent periods of reactivation in 7×10^{-6} Torr of oxygen at 1120 K.

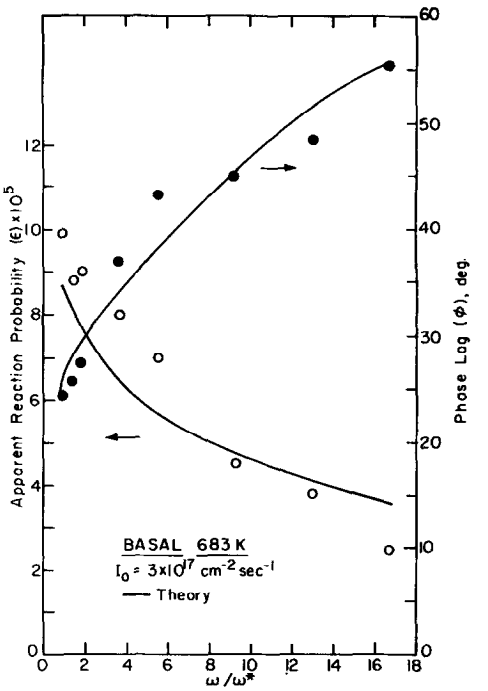

FIG. 5. Frequency scan of basal plane specimens at the reference temperature and beam intensity.

platinum strips. At high coverage, the size of the platinum zones is probably larger than at low platinum coverage and consequently more time is required to deactivate the metal surface. Modeling the metal zones in Fig. 1 as strips of half-width L_{Pt}, the characteristic time for surface diffusion of carbon-bearing impurities from the edge of the strip inward is L_{Pt}^2/D_{sC}, where D_{sC} is the surface diffusivity of the poisoning impurity on platinum. Taking $L_{Pt} \sim 100$ Å and a deactivation time of ~ 1 hr (Fig. 4, for four equivalent monolayers coverage), the surface diffusivity of the poisoning species is between 10^{-15} and 10^{-16} cm^2/sec at ~ 700 K. If the poisoning were due to impurities arriving from the background gas (pressure $= 7 \times 10^{-9}$ Torr) the time to produce a noticeable poisoning effect should have been independent of platinum coverage. The dashed segments of the upper and lower curves in Fig. 4 represent 10-min oxygen treatment periods, which appear to have been sufficient to return the samples to their initial reactivity.

Figures 5, 6, and 7 show the results of the experiments on the basal specimen coated with four equivalent monolayers of platinum in which modulation frequency, incident H_2 beam intensity, and solid temperature were varied from the reference conditions. The curves marked "Theory" are the results of fits to a reaction model, which will be presented later. Over a modulation frequency variation of a factor of 16, the phase lag on the basal plane specimen rises from 24 to 57° and the reaction probability decreases by a factor of ~ 3 (Fig. 5). For the beam intensity variation shown in Fig. 6, the phase lag changes by only a few degrees but the apparent reaction probability varies by a factor of ~ 4. The results of the temperature variation experiments (Fig. 7) indicate a rather temperature-insensitive phase lag of $\sim 27°$ and a reaction probability which attains a maximum at ~ 680 K. These results are generally similar to those obtained in Ref. (*1*) with atomic hydrogen on basal plane graphite except that the phase lags are somewhat larger in the present case and the reaction probability is smaller and exhibits a maximum not seen in the C/H system.

The corresponding results for prism plane specimens with four equivalent monolayers of platinum are shown in Figs. 8–10. The features of these plots are generally similar to those on the basal plane specimens with the very significant exception of the insensitivity of the phase lag to modulation frequency seen in Fig. 8.

IV. SURFACE REACTION MODEL

Our first attempt at explaining the results shown in Figs. 5–10 consisted in accepting *in toto* the reaction mechanism developed for the C/H system (*1*) and simply treating the platinum as a means of producing a non-zero dissociative sticking probability for H_2 on graphite. Cal-

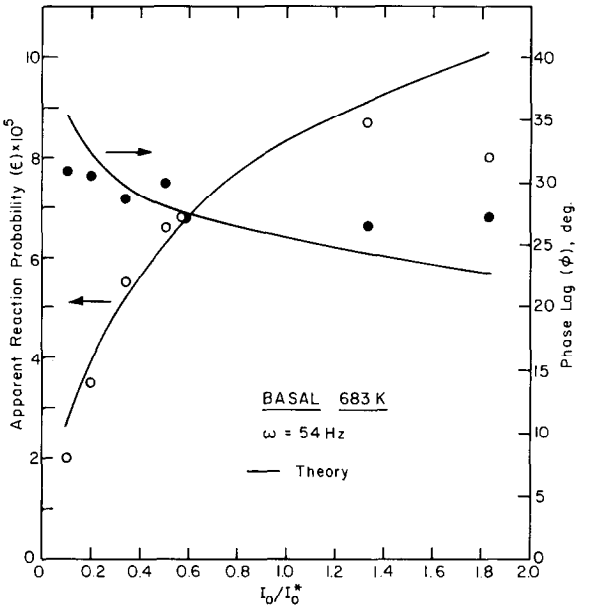

FIG. 6. Effect of beam intensity on the basal plane gasification reaction at the reference temperature and modulation frequency.

culations based on this model were performed for the prism specimen at 683 K with the sticking probability varied until the magnitude of the reaction probabilities agreed roughly with those shown on Figs. 8 and 9. This calculation, however, produced phase lags which were 15 to 20° higher than those observed (Figs. 8 and 9) and reaction probabilities which depended much more strongly on beam intensity than what was observed. Since a 15 to 20° phase lag error constitutes a massive failure

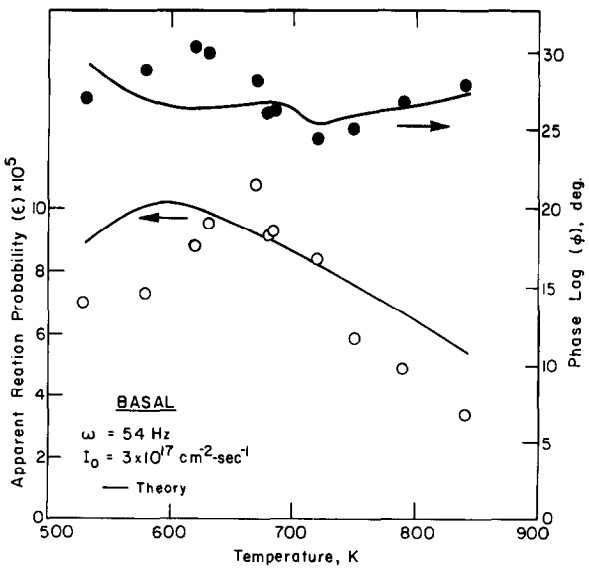

FIG. 7. Effect of temperature on the basal plane reaction probability and phase lag at the reference frequency and beam intensity.

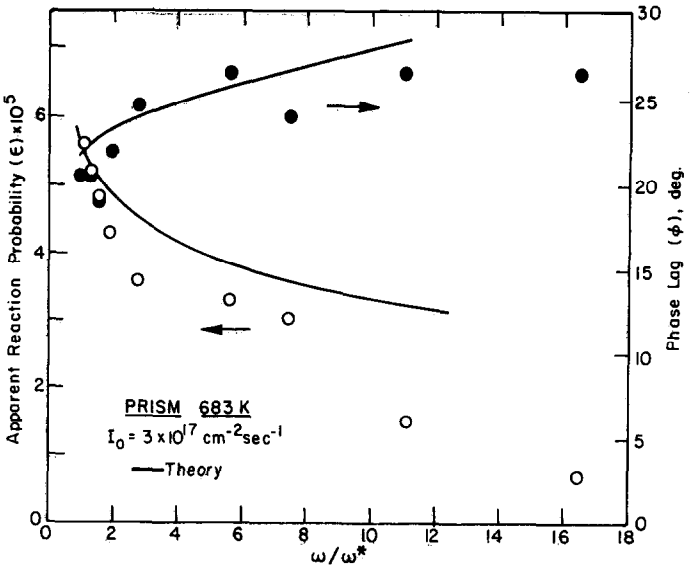

FIG. 8. Frequency scan of prism plane specimens at the reference temperature and beam intensity.

of a model, we concluded that the present results cannot be matched simply by changing the value of the sticking probability of the incident hydrogen on the surface.

In searching for a detailed mechanistic interpretation of the platinum-catalyzed reaction, the role of the platinum zones seen in Fig. 1 had to be specified. Are they the sole supplier of atomic hydrogen to the adjacent graphite surface or does the exposed graphite contain sufficient very finely (even atomically) dispersed platinum which is not visible in the photomicrographs but which actually catalyzes the reaction? The latter explanation was rejected for several reasons. First, if it were true, the model used for the C/H reaction should have been capable of rationalizing the C/Pt/H_2 results. As dis-

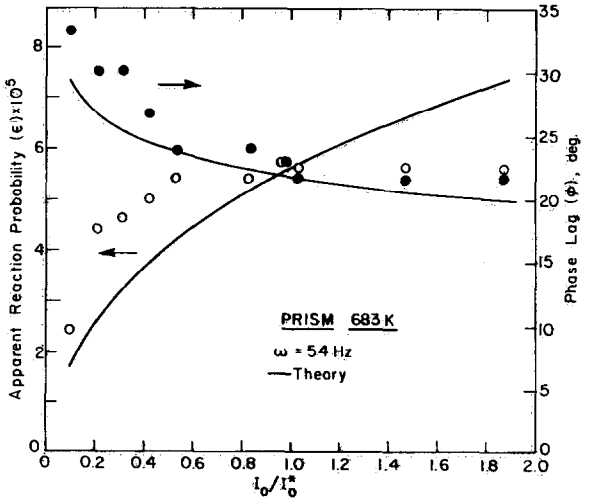

FIG. 9. Effect of beam intensity on the prism plane gasification reaction at the reference temperature and modulation frequency.

cussed above, such accord could not be obtained. Second, if atomically dispersed platinum on what appears to be the graphite parts of the surface were responsible for the reaction, four equivalent monolayers of platinum should not have been required to reach maximum reactivity. Instead, the reaction should have started abruptly with a fraction of a monolayer of platinum; further metal deposition should simply have grown the second-phase platinum zones without increasing the concentration of platinum atoms on the graphite. Third, it is unlikely that atomically dispersed platinum on the exposed graphite surfaces would have inverted the normal order of reactivity of the two orientations of pyrolytic graphite. The decrease in reaction probability with increasing temperature (Figs. 7 and 10), which reflects the instability of methane compared with H_2, occurs at about the same temperatures as in the C/H system (*1*). This observation suggests that the ratio of the methane formation rate to the H atom recombination rate on graphite is not affected by the presence of platinum. Finally, a nearly frequency-independent phase lag (Fig. 8) cannot be obtained from the original C/H reaction model. Such behavior is best explained by two back-to-back diffusional processes, which is not part of the earlier model.

Consequently, we conclude that the platinum zones seen in Fig. 1 play an essential role in the reaction mechanism, or that the reaction is heterogeneous on the scale of the surface morphology. The basic idea of the mechanism is simple: Incident H_2 is dissociatively adsorbed on the platinum zones but merely scatters from the graphite part of the surface. Some of the hydrogen chemisorbed on the platinum zones recombines and is re-emitted to the gas phase as H_2. The remainder of the chemisorbed hydrogen spills over onto the adjacent graphite and proceeds to diffuse along the surface and

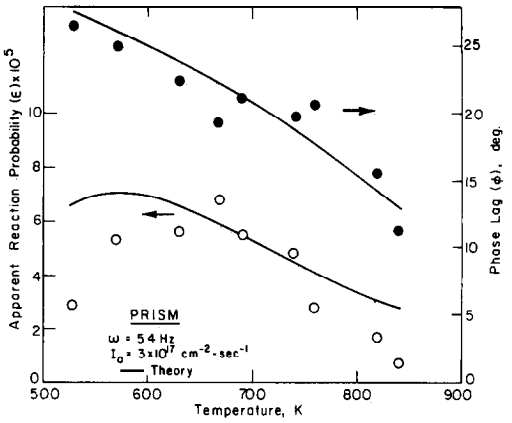

FIG. 10. Effect of temperature on the prism plane reaction probability and phase lag at the reference frequency and beam intensity.

simultaneously react (either by methane production or by recombination) and dissolve and migrate in the bulk graphite.

Although the basic features of the model are clear, the details are not. First, if surface diffusion on the graphite is important, must surface diffusion of adsorbed hydrogen on the platinum be considered? We have found that for reasonable fitting of the data, surface migration of H atoms must be considered on the graphite but not on the platinum. Second, should the spill-over of H atoms from the platinum zones to the graphite be treated as an irreversible step or as an interfacial equilibrium? Data fitting attempts employing these two limiting cases indicated that interfacial equilibrium is preferable.

The model which evolved from these preliminary analyses is depicted in Fig. 11. The platinum and graphite zones of the surface are modeled as infinitely long strips of half-widths L_{Pt} and L_C, respectively. This geometric simplification receives some support from the appearance of the two phases on Fig. 1 and is much easier to treat mathematically than circular islands of platinum. The sticking process on the platinum strips is assumed to be coverage-dependent because no other way could be found to reproduce the maxima in the

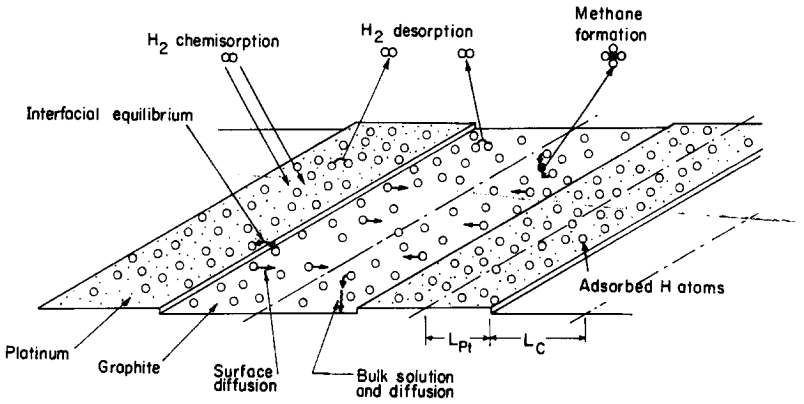

FIG. 11. Schematic of the reaction model.

reaction probabilities observed in Figs. 7 and 10. Some of the adsorbed hydrogen recombines on the platinum. The population of H atoms adsorbed on the platinum equilibrates with the H adatoms on the graphite surface at the boundary between the two surface phases. Once on the graphite surface, the adsorbed hydrogen is subject to the same elementary processes as if it were on pure graphite, having arrived there directly from gas phase atomic hydrogen. In addition, because the supply of hydrogen on the graphite strip is located at the C/Pt interface, surface diffusion occurs simultaneously with surface reaction and bulk solution-diffusion. Gas phase H_2 does not chemisorb directly on the exposed graphite.

Quantitative treatment of the model consists of writing balance equations for each distinct surface species on (or in) each phase. In the present case, there is only one species, atomic hydrogen. There are three phases: the platinum, the graphite surface, and the bulk graphite. The balance equations are time-dependent because of modulation of the primary reactant beam. Because of the diffusional processes occurring in and on the graphite, the balance equations for these two phases assume the form of transient diffusion equations. The chemical reactions which take place on the graphite surface appear as sink terms in this balance, which unfortunately renders the differential equations nonlinear. The three balance equations are solved by Fourier expansion in the time variable, with only the zeroth order and fundamental mode solutions retained. The rate of methane formation on the graphite is expressed in terms of the H atom concentration and the rate of H_2 emission from the entire surface is similarly formulated. The H_2 flux from the surface provides the reference signal against which the methane signal is compared. The H_2 emitted from both zones of the surface contains contributions due to direct scattering of the incident beam and to the recombination steps which are part of the mechanism. The rates of CH_4 and H_2 emission are Fourier analyzed and the quotient of the fundamental modes is formed. This quantity is the reaction product vector which gives the theoretical apparent reaction probability and phase lag for comparison with the data. The parameters of the reaction model consist of the rate constants of the elementary steps of which the model is composed. Computer optimization is used to select values of these parameters which provide the best agreement between theory and data.

The H atom balances on the two surface phases are written for the unit cell

consisting of a unit length of half of a graphite strip and half of a platinum strip.

H Atom Balance on Platinum

$$\frac{dm}{dt} = 2\eta I_0\left(1 - \frac{m}{N_s}\right)^2 g(t) - 2k_{Pt}m^2 + \frac{D_s}{L_{Pt}}\left(\frac{\partial n}{\partial x}\right)_{x=0} \quad (1)$$

where:

m = surface concentration of H on Pt, atoms/cm^2
t = time, sec
η = bare surface sticking probability of H_2 on Pt
I_0 = amplitude of modulated H_2 beam, molecules/cm^2-sec
N_s = density of adsorption sites for H_2 on Pt, cm^{-2}
$g(t)$ = gating function (time variation) of the incident beam
k_{Pt} = rate constant for H atom recombination and desorption as H_2 (on platinum), cm^2/sec
D_s = surface diffusion coefficient of H atoms on the graphite surface, cm^2/sec
L_{Pt} = half-width of platinum strip, cm (equal to the area of platinum in a unit cell of 1 cm length)
x = distance from the Pt/C interface measured into the graphite strip, cm
n = surface concentration of H atoms on the graphite, atoms/cm^2.

The first term on the right hand side of Eq. (1) represents chemisorption of hydrogen from the incident beam on the platinum part of the unit cell. The sticking probability is taken to vary with the square of the fraction of available sites, in accord with the results of Lu and Rye (*2*). The next term represents loss of H atoms due to recombination on the platinum surface. At the temperatures utilized in the experiments, molecular desorption is certain to be much larger than atom evaporation (*4*), so second order desorption kinetics are appropriate (*2*). The last term in Eq. (1) represents the spill-over of adsorbed hydrogen to the graphite surface. This loss term in equal to the diffusive flux of H atoms away from the Pt/C interface on the graphite surface.

H Atom Balance on the Graphite Surface

$$\frac{\partial n}{\partial t} = D_s\frac{\partial^2 n}{\partial x^2} - 2k_C n^2 - 4k_R n^3 + D_v\left(\frac{\partial c}{\partial z}\right)_{z=0} \quad (2)$$

where:

k_C = second order desorption rate constant for H atom recombination on graphite, cm^2/sec.
k_R = rate constant for methane formation on graphite, cm^4/sec (in Ref. (*1*), this rate constant was expressed as the product of the equilibrium constants for reactions leading to CH_2 and the rate constant for attachment of an H atom to this species)
D_v = bulk diffusion coefficient of H atoms in graphite, cm^2/sec
z = distance beneath the graphite surface, cm
c = concentration of H atoms in bulk graphite, atoms/cm^3.

The first term on the right hand side of Eq. (2) represents surface diffusion of hydrogen on graphite. The last term gives the drain on the population of adatoms due to solution and diffusion in the bulk.

H Atom Balance in the Bulk Graphite

$$\frac{\partial c}{\partial t} = D_v\frac{\partial^2 c}{\partial z^2} \quad (3)$$

Based upon the assumption of interfacial equilibrium, the following laws of mass action apply:

$$n(0, t) = H_s m(t) \tag{4}$$

at the Pt/C interface, and

$$c(x, 0, t) = H_v n(x, t) \tag{5}$$

between atomic hydrogen adsorbed on the graphite surface and dissolved in the bulk graphite. H_s and H_v are the distribution coefficients characterizing these two equilibria.

The three H atom balances are coupled at the phase boundaries by Eqs. (4) and (5). At the other boundaries, the conditions are:

$$\left(\frac{\partial n}{\partial x}\right)_{x=L_C} = 0 \tag{6}$$

$$c(x, \infty, t) = 0 \tag{7}$$

where:

L_C = half-width of the graphite strip in the unit cell.

Equation (6) is a result of symmetry about the middle of the graphite strip.

The theoretical apparent reaction probability and phase lag for this model of the surface reaction is presented in Ref. (*6*). These calculated quantities are to be compared with the data in Figs. 5–10. Such a comparison requires selection of all of the physicochemical parameters describing each elementary step of the model, which are summarized below.

Geometrical: L_C and L_{Pt}
Pt/H_2 interaction: η, N_s, k_{Pt}
Interfacial equilibrium: H_s
Graphite/H interaction:
k_R, k_C, $H_v D_v^{\frac{1}{2}}$, D_s.

The object is to choose values of these parameters and their temperature dependences so that the variation of ϵ and ϕ with the experimentally controllable variables ω, I_0, and T provides the best agreement of the theory with the data.

The data fitting process is divided into two stages. First, the data obtained with frequency and beam intensity as variables (e.g., Figs. 5 and 6 for the basal plane) are utilized to determine the best parameter values at a single temperature. Second, the data taken over a range of temperatures are used to determine the activation energies of as many of the rate constants as possible.

V. DETERMINATION OF REACTION PARAMETERS

If some of the parameters in the above list can be fixed in advance, the fitting procedure gives more reliable values of the remaining ones than if all parameters are allowed to float in the fitting process. Thus, L_C and L_{Pt} were estimated from the electron micrographs of Fig. 1. These dimensions were estimated to be:

L_C = 50 Å and L_C/L_{Pt} = 0.5 (basal)

L_C = 100 Å and L_C/L_{Pt} = 1.0 (prism)

Inasmuch as the proposed reaction model assumes that the graphite portions of the surface are free of platinum, the methane formation and hydrogen desorption rate constants should be the same as those determined in the C/H study of Ref. (*1*). For the basal plane:

$$k_C = 1.3 \times 10^{-4} \times \exp(-18.5/RT) \text{ cm}^2/\text{sec} \tag{8}$$

$$k_R = 2.2 \times 10^{-21} \times \exp(0.9/RT) \text{ cm}^4/\text{sec} \tag{9}$$

and for the prism plane:

$$k_C = 1.1 \times 10^{-4} \times \exp(-15.9/RT) \text{ cm}^2/\text{sec} \tag{10}$$

$$k_R = 1.3 \times 10^{-18} \times \exp(-3.3/RT) \text{ cm}^4/\text{sec} \tag{11}$$

where the activation energies are in kcal/mol.

We found that acceptable agreement between the model predictions and the data could not be achieved if the parameters representing bulk solution and diffusion of hydrogen in graphite $[H_vD_v^{\frac{1}{2}}]$ were fixed at the value deduced from the C/H study of Ref. (*1*). However, such consistency should not be expected because the bulk properties of pyrolytic graphite are very sensitive to the fabrication and heat treatment processes used in preparing the material. Although the graphite specimens used in the present study were nominally the same as those employed in C/H investigation, they were not from the same lot. In accepting the values of k_R and k_C from Ref. (*1*), however, we have assumed that the surface properties of the graphites (after polishing) are the same for both lots. To allow for variability of the bulk properties, the solution–diffusion parameter was permitted to be a free variable:

$$H_vD_v^{\frac{1}{2}} = [H_vD_v^{\frac{1}{2}}]_0 \times \exp(-E_{H_vD_v}/RT) \quad (12)$$

The remaining parameters were allowed to be totally free:

$$k_{Pt} = (k_{Pt})_0 \exp(-E_{Pt}/RT) \quad (13)$$

$$H_s = (H_s)_0 \exp(-E_{H_s}/RT) \quad (14)$$

$$D_s = (D_s)_0 \exp(-E_{D_s}/RT) \quad (15)$$

The bare surface sticking probability η is unknown but assumed to be temperature independent. The active site density N_s is a secondary quantity because it affects only the coverage dependence of the sticking probability and was important only for the lowest temperature points of Figs. 7 and 10.

Thus, 10 parameters were obtained from the data of Figs. 5–7 for the basal plane specimen. The best values were chosen by the optimization routine MINUIT, which compares all of the data with the theoretical reaction model. Five of the parameters, the 683 K values of $H_vD_v^{\frac{1}{2}}$, k_{Pt}, H_s, D_s, and η were determined from the data on Figs. 5 and 6. The remaining five parameters, namely the four activation energies and the site density on the platinum surface, were obtained from the data on Fig. 7. The prism plane data in Figs. 8–10 were similarly analyzed. The results are summarized in Table 1.

VI. DISCUSSION

The values of the graphite bulk solution/diffusion parameter $H_vD_v^{\frac{1}{2}}$ inferred from the present study are considerably different from those determined in the C/H study (*1*). At 683 K, the values $H_vD_v^{\frac{1}{2}}$ deduced from the present data are 20 to 40 times larger than those obtained earlier and the activation energies (which are the sum of the solution en-

TABLE 1

Reaction Parameters for Hydrogen Gasification of Platinum-Covered Graphite

Parameter	Value at 683 K		Preexponential factor		Activation energy, (kcal/mol)	
	Basal	Prism	Basal	Prism	Basal	Prism
$H_vD_v^{\frac{1}{2}}$ ($sec^{-\frac{1}{2}}$)	1.3×10^4	8.7×10^4	4300	1500	−1.5	−5.5
k_{Pt} (cm^2/sec)	5.7×10^{-10}	4.6×10^{-8}	8×10^{-6}	9×10^{-2}	13.0	19.7
H_s	0.16	0.34	1.1	21	2.6	5.6
D_s (cm^2/sec)	4×10^{-10}	9×10^{-10}	6×10^{-5}	6×10^{-7}	15.1	8.8
N_s (cm^{-2})	4×10^{13}	4×10^{13}	—	—	—	—
η	0.04	0.09	—	—	—	—

thalpies of H_v and one-half of the activation energies of D_v) are negative rather than positive. As discussed in the previous section, many properties of pyrolytic graphite are very sensitive to fabrication history. In addition, it is conceivable that some platinum is absorbed between basal planes in the graphite and alters its bulk properties (i.e., the solubility and diffusivity of hydrogen).

The desorption activation energies of hydrogen on platinum (E_{Pt} = 13 kcal/mol for Pt deposited on the basal plane and 19.7 kcal/mol for Pt on the prism plane) compare reasonably well with the value of 17.5 kcal/mol determined by Lu and Rye's flash desorption experiments on bulk single crystals of platinum (*2*). The preexponential factor for the recombination process of H atoms on the platinum zones in the present experiment, however, depends strongly on the orientation of the graphite substrate. For platinum on the basal plane of graphite, $(k_{Pt})_0 = \sim 10^{-5}$ cm^2/sec while on the prism plane specimen, the corresponding value is $\sim 10^{-1}$ cm^2/sec. The expected value for a surface bimolecular reaction of this type is 10^{-2} cm^2/sec (*6*). It is difficult to avoid the interpretation of very different hydrogen desorption rate constants for the platinum on the two graphite surfaces; the variation of methane phase lag with modulation frequency shown in Figs. 5 and 8 is determined primarily by k_{Pt}, and the data show a distinct difference between the two orientations of the substrate in this regard. As long as the reaction model contains dissociative adsorption and desorption from platinum zones as principal features, the factor of 100 difference in k_{Pt} at 683 K shown in Table 1 is a consequence. The only physical justification of the different H atom recombination rate constants on the platinum on the two graphite surfaces is that because the layers are very thin (four to eight monolayers), they exhibit epitaxy with the substrate. The platinum layers on the two forms of graphite may therefore have different interatomic spacings and even different crystal structures, which could account for the different rate constants for surface H atom recombination. In this regard, it should be noted that the substrate which supported the thickest deposit (the prism orientation) showed a preexponential factor and an activation energy closer to what is expected from bulk platinum than did the thinner deposit on the basal plane.

The values of the platinum/graphite interfacial equilibrium constant H_s shown in Table 1 can be interpreted in simple statistical mechanical terms. The mass action law of Eq. (4) refers to the equilibrium:

$$\mathrm{H(Pt)} \rightleftharpoons \mathrm{H(C)} \tag{16}$$

The quantity E_{H_s} of Eq. (14) is the difference in the binding energies of hydrogen atoms on the two surfaces:

$$E_{H_s} = \chi_{Pt} - \chi_C \tag{17}$$

The values of E_{H_s} shown in Table 1 are positive, which means that the hydrogen is more strongly bound on the platinum surface than on the graphite surface. The H atom binding energies are related to the activation energies for surface recombination which yields molecular hydrogen according to (*7*):

$$\chi = \tfrac{1}{2}(D + E) \tag{18}$$

where D is the bond energy of H_2. Substituting Eq. (18) into Eq. (17) gives the relation between E_{H_s} and the activation energies for hydrogen atom recombination on the two surfaces:

$$E_{H_s} = \tfrac{1}{2}(E_{Pt} - E_C) \tag{19}$$

The values of E_{Pt} determined from the present study are the activation energies of the rate constants k_{Pt} given in Table 1. The activation energies E_C for the two graphite surfaces obtained from the C/H study of Ref. (*1*) are contained in Eqs.

(8) and (10). Using these values in Eq. (19) yields predicted values of E_{H_s} of -2.8 and 1.9 kcal/mol for the basal and prism planes, respectively. The observed values shown in Table 1 are 4 to 5 kcal/mol larger, being 2.6 kcal/mol for the basal specimens and 5.6 kcal/mol for the prism surface.

The preexponential factor of H_s can be estimated theoretically if the states of the adsorbed hydrogen on the platinum and graphite surfaces are known. The procedure is a straightforward application of the method outlined by Ehrlich (7) for chemisorption from the gas phase. To represent interfacial equilibrium, the chemical potentials of hydrogen on the platinum and graphite surfaces, which are computed from the partition functions of the adsorbed states, are equated. If the H atom populations are localized on both surfaces, the preexponential factor of H_s is found to be:

$$(H_S)_0 = \frac{(N_S)_C}{(N_S)_{Pt}} \frac{(z_\perp)_C}{(z_\perp)_{Pt}} \frac{(z_{||})_C^2}{(z_{||})_{Pt}^2} \qquad (20)$$

where N_s is the density of adsorption sites and z_0 denotes a vibrational partition function referenced to the ground state:

$$z = \left[1 - \exp\left(-\frac{h\nu}{kT}\right)\right]^{-1} \qquad (21)$$

where ν is the frequency of vibration, h is Plank's constant, and k is the Boltzmann constant. The subscript $\perp$ denotes vibration prependicular to the surface and $||$ designates the two degrees of freedom for vibration parallel to the surface.

If the adsorbed hydrogen on both surfaces is best represented by the two-dimensional ideal gas model instead of localized vibrators, the preexponential factor of H_s would be equal to the middle ratio on the right hand side of Eq. (20). Because of the significant activation energy for surface diffusion of H on graphite (Table 1), the localized adsorption limit is more appropriate than the ideal two-dimensional gas limit. On metal surfaces, the activation energy for adatom surface migration is 10 to 20% of the binding energy χ (7); this rule-of-thumb yields an activation energy of surface diffusion of hydrogen atoms on platinum of $\sim$10 kcal/mol, which would suggest localized adsorption on this surface as well. Consequently, it is appropriate to compare the experimental values of $(H_S)_0$ with Eq. (20). If the adsorbed H atoms are in their lowest vibrational states on both surfaces (i.e., $h\nu \gg kT$), the partition functions are unity. If in addition, the site densities on the two surfaces are approximately equal, Eq. (20) shows that $(H_S)_0$ should be about unity. This prediction agrees with the value shown in Table 1 for the basal specimen. On the prism specimen, the observed value of $(H_S)_0$ is $\sim$20, which may be due to a combination of a higher adsorption site density or population of higher vibrational states on the prism face of graphite compared to the surface of the platinum deposited on this face.

The preexponential factors of D_s are $\sim 10^{-4}$ cm^2/sec for basal plane graphite and $\sim 10^{-6}$ cm^2/sec for the prism specimen. The latter is considerably smaller than the value obtained for oxygen on molybdenum (8) and fluorine on UO_2 (9), both of which are $\sim 10^{-4}$ cm^2/sec. The activation energies for surface diffusion of hydrogen on graphite are 15 and 9 kcal/mol for the basal and prism planes, respectively. Both of these values are considerably smaller than Robell's measurement of 39 kcal/mol on ordinary graphite for temperatures between 300 and 400°C (10). At 683 K, Robell's data gives $D_s \simeq 10^{-16}$ cm^2/sec, which is quite a bit smaller than the values of 4×10^{-10} to 9×10^{-10} cm^2/sec we obtained at this temperature.

The site density of 4×10^{13} cm^{-2} determined from the low temperature experiments is a factor of 10 smaller than the value inferred from the flash desorp-

tion experiments of Lu and Rye (*2*). However, this discrepancy is in the direction expected; considerable care is taken to achieve carbon-free single crystal surfaces in order to obtain the site density of 4×10^{14} cm^{-2} they obtained. In our experiments, the finely dispersed platinum is surrounded by carbon, and the oxygen treatment given the specimens probably did not completely remove all of the carbon impurities from the surface.

The bare surface sticking probabilities of H_2 on Pt shown in Table 1 are smaller than the value of ~ 0.3 which can be achieved on clean single crystal platinum (*2*, *5*). The bare surface sticking probability can be regarded as the product of the density of adsorption sites and the area per site, or

$$\eta = \sigma N_s \qquad (22)$$

where σ is the area of the platinum surface rendered inactive to chemisorption if a site is occupied by an adsorbed hydrogen atom. Using the site densities and sticking probabilities from Table 1, the diameter of the deactivated zone around an adatom, $(4\sigma/\pi)^{\frac{1}{2}}$, is 3.6 and 5.3 Å for platinum on the basal and prism substrates, respectively. These values may be compared to the corresponding values on the low index planes of bulk single crystal platinum, which range from 1.0–3.2 Å (*2*).

VI. CONCLUSIONS

The model proposed for the platinum-catalyzed gasification of pyrolytic graphite by molecular hydrogen is based upon chemisorption of H_2 platinum zones on the surface followed by spill-over of hydrogen to the adjacent graphite. Here, the reactions which take place are the same as those which predominate when hydrogen is supplied to pure graphite surfaces from gas phase atomic hydrogen. Both surface diffusion and bulk solution/diffusion occur simultaneously with the surface reactions on the graphite surface. Quantitative predictions based upon this model provide a good fit to molecular beam data for the partially platinum-covered basal and prism planes of graphite and yield values of the rate constants of the elementary steps in the mechanism which appear to be reasonable.

REFERENCES

1. Balooch, M., and Olander, D. R., *J. Chem. Phys.* **63**, 4772 (1975).
2. Lu, D. E., and Rye, R. R., *Surf. Sci.* **45**, 677 (1974).
3. Norton, P. R., and Richards, P. J., *Surf. Sci.* **41**, 293 (1974).
4. Bernasek, S. L., and Somorjai, G. A., *J. Chem. Phys.* **62**, 3149 (1975).
5. Salmeron, M., Gale, R., and Somorjai, G. A., *J. Chem. Phys.* **70**, 2807 (1979).
6. Baetzold, R. C., and Somorjai, G. A., *J. Catal.* **45**, 94 (1976).
7. Ehrlich, G., *J. Chem. Phys.* **31**, 1111 (1959).
8. Ullman, A. Z., and Madix, R. J., *High Temp. Sci.* **6**, 342 (1974).
9. Machiels, A. J., and Olander, D. R., *High Temp. Sci.* **9**, 3 (1977).
10. Robell, A., Ph.D. Thesis, University of California, Berkeley (1964).